JOURNAL PRE-PROOF

This is an early version of the article, published prior to copyediting, typesetting, and editorial correction. The manuscript has been accepted for publication and is now available online to ensure early dissemination, author visibility, and citation tracking prior to the formal issue publication.



It has not undergone final formatting or technical editing by the journal's editorial team. Content is subject to change in the final Version of Record.

To differentiate this version, it is marked as **"PRE-PROOF PUBLICATION"** and should be cited with the provided DOI. A visible watermark on each page indicates its preliminary status.

The final version will appear in a regular issue of JPPR, with final metadata, layout, and pagination.

Please cite this article as:

Moreno-López J.P., Méndez-Pineda D.O., Marroquín-Martínez L.P., Giraldo-Álvarez L.J., Banda-Sánchez L. del C. Epidemiological patterns of black pod (*Phytophthora* spp.) and frosty pod rot (*Moniliophthora roreri*) in cocoa plantations of Tequendama, Colombia. Journal of Plant Protection Research. DOI: 10.24425/jppr.2026.8031

Original article

Epidemiological patterns of black pod (*Phytophthora* spp.) and frosty pod rot (*Moniliophthora roreri*) in cocoa plantations of Tequendama, Colombia

Jenny Paola Moreno-López[1, 2], Diego Orlando Méndez-Pineda[2], Laura Paola Marroquín-Martínez[2], Laura Julieth Giraldo-Álvarez[2], Laguandio Del Cristo Banda-Sánchez[2]

[1] Faculty of Agricultural Sciences, Universidad Nacional de Colombia, Carrera 45 No. 26-85, 111311, Bogotá, Colombia

[2] Department of Agricultural Engineering – Faculty of Agricultural Sciences, Universidad de Cundinamarca, Manuel Humberto Cárdenas, 25290, Fusagasuga, Colombia

***Corresponding address:** jpmoreno@ucundinamarca.edu.co

Received: March 20, 2026

Accepted: October 15, 2026

Online Pree-Proof Publication: November 2, 2026

Responsible Editor: Kallol Das

DOI: 10.24425/jppr.2026.8031

PRE-PROOF PUBLICATION

PRE-PROOF PUBLICATION JOURNAL OF PLANT PROTECTION RESEARCH

Abstract

Cocoa is an important crop in Colombia and a key productive alternative in post-conflict rural areas. Similar to other tropical production systems, yields are constrained by diseases such as black pod disease and frosty pod rot. This study evaluated the temporal and spatial epidemiological patterns of both diseases on three cocoa farms located in the Tequendama region of Colombia through analyses of disease incidence, severity, disease progress, and spatial distribution. Pod assessments were conducted over a six-month period, recording disease incidence, severity, pod developmental stage, and canopy stratum. Temporal analyses evaluated the effects of temperature and relative humidity on disease incidence, whereas spatial analyses examined disease distribution among farms and canopy strata and assessed horizontal spatial autocorrelation using Moran's I. The results revealed contrasting epidemiological patterns. Black pod incidence was not significantly associated with temperature or relative humidity and remained low throughout the study period. Incidence increased from the lower to the upper canopy layer, and most variability occurred among trees rather than among farms. In contrast, frosty pod rot showed significant negative associations with temperature and relative humidity and consistently there was a higher incidence in the upper canopy layer. Severity and AUDPC values were also greater for frosty pod rot than for black pod disease. Moran's I analyses did not detect significant spatial autocorrelation at the farm scale. These findings demonstrated that black pod disease and frosty pod rot differed in their temporal dynamics and canopy distribution patterns despite affecting the same host organ. The results highlighted the importance of disease-specific epidemiological approaches and provided information relevant for improving disease monitoring and management in cocoa production systems.

Keywords: AUDPC, epidemiology, incidence, severity, *Theobroma cacao*

PRE-PROOF PUBLICATION

PRE-PROOF PUBLICATION JOURNAL OF PLANT PROTECTION RESEARCH

Introduction

Cocoa (*Theobroma cacao* L.) is a tropical crop on which many rural families worldwide depend economically, with its seeds constituting the primary raw material for chocolate production. In 2022, global cocoa production reached 4.82 million tons, benefiting multiple actors along the value chain, particularly smallholder farmers (Kongor *et al*. 2024).

According to reports from the National Federation of Cocoa Growers (FEDECACAO, 2024), approximately 65,000 families in Colombia depend on cocoa production. This crop plays an important role in economic and social development programs aimed at promoting peace in regions historically affected by armed conflict. It also serves as a key component in the substitution of illicit crops, contributing to improved living conditions in rural communities. Current national production exceeds 60,000 tons of dried cocoa beans annually (Charry *et al*. 2025; Rodríguez-Medina *et al*. 2019).

The department of Cundinamarca ranks seventh in Colombia's cocoa production (León *et al*. 2023), with a planted area of 7,650 hectares, where cocoa production has expanded as a viable alternative for smallholder farmers in several regions, including Tequendama (Government of Cundinamarca, 2025). As in other cocoa-producing areas of the country (Hernández-Núñez *et al*. 2025), cocoa in the Tequendama region is managed through agroforestry systems, typically on farms of less than three hectares. Production is generally carried out by smallholder farmers with low levels of inputs and limited technological resources, and a predominance of agroforestry systems using shade trees and family labor (Rojas *et al*. 2014). Crop management practices are similar to those employed by cocoa producers in other producing regions around the world (Kongor *et al*. 2024).

Cocoa production in major producing countries is threatened by diseases such as black pod, caused by several *Phytophthora* species including *Phytophthora palmivora* E.J. Butler, *Phytophthora capsici* Leonian, and *Phytophthora citrophthora* (R.E. Sm. & E.H. Sm.) Leonian, among others, and frosty pod rot caused by

Moniliophthora roreri (Cif.) H.C. Evans. These diseases are among the most limiting factors affecting cocoa production in Colombia and can occur at any stage of pod development (Vanegas *et al*. 2026; Lopez-Torres *et al*. 2025; Jibat and Alo 2023; Mora and Fiallos 2012). Yield losses can exceed

90%, depending on agroecological conditions and crop management practices in the production area (Ramírez-Martínez *et al*. 2021). The importance of phytosanitary monitoring in

PRE-PROOF PUBLICATION

PRE-PROOF PUBLICATION JOURNAL OF PLANT PROTECTION RESEARCH

cocoa production systems lies in quantifying the incidence and severity of diseases, understanding their epidemiological dynamics, and developing predictive models that help reduce yield constraints. In this context, effective and systematic monitoring of diseases such as moniliasis and black pod in cocoa provides key information for identifying critical infection periods and optimizing integrated management strategies (Bailey & Meinhardt 2016; Correa-Álvarez *et al*. 2014). Likewise, various studies have shown that microclimatic variables such as temperature, relative humidity, and precipitation significantly influence the onset and progression of these diseases; therefore, joint monitoring allows for the development of prediction tools adapted to local agroecological conditions (Leandro-Muñoz *et al*. 2017). The objective of this study was to evaluate the spatial and temporal dynamics of black pod and frosty pod rot on cacao farms located in the Tequendama region (Colombia).

Materials and Methods

Study area

Disease assessments were conducted on three cocoa farms located in the municipality of Viotá, Tequendama province (Cundinamarca, Colombia): La Marina (4°24′13″ N, 74°30′22″ W), with 500 cocoa trees, El Rubí (4°25′16″ N, 74°30′45″ W) with 150 cocoa trees, and El Castillo (4°24′26″ N, 74°29′53″ W) with 120 cocoa trees, located in the rural districts of La Florida and Brasil Bajo (Figure 1). The study area was located at an average altitude of 575 m above sea level, with temperatures ranging from 23°C to 32°C depending on rainfall seasonality. Annual precipitation ranged between 850 and 1,600 mm, and relative humidity averaged approximately 65% during the dry season. Multiple hybrid commercial cocoa clones of diverse genetic origin were cultivated on these farms.

Morphological identification of phytopathogens isolated from symptomatic pods

To perform a morphological identification of the phytopathogens associated with the symptoms observed under field conditions, up to the genus level, samples of diseased cocoa pods were collected, individually stored in sealed bags, and transported in portable coolers to the microbiology laboratory at the Universidad de Cundinamarca for processing. For pathogen isolation, potato dextrose agar (PDA), malt extract agar (MEA), and V8 agar supplemented with chloramphenicol (0.1 g l^{-1}) were used. Pod samples were washed with running water. Tissue

PRE-PROOF PUBLICATION
PRE-PROOF PUBLICATION JOURNAL OF PLANT PROTECTION RESEARCH

explants were obtained, and surface sterilization was performed using 2.5% sodium hypochlorite for one minute, followed by three rinses with sterile distilled water (Moreno-López *et al*. 2022; Hipólito-Romero *et al*. 2020). Pathogenicity tests were conducted on detached cocoa pods to verify that the isolates morphologically identified as *Moniliophthora* sp. and *Phytophthora* spp. were the causal agents associated with the disease symptoms observed in the field (Abad *et al*. 2023; Alsutan *et al*. 2022; Maridueña-Zabala *et al*. 2021; Villamizar-Gallardo *et al*. 2019).

Sampling of black pod and frosty pod rot

Symptoms of frosty pod rot and black pod were visually identified on the three selected farms. Five sampling events were conducted over a six-month period, except for the El Castillo farm, where three sampling visits were performed. The evaluation period was designed to encompass at least one complete harvest cycle, corresponding to approximately 150–180 days of active pod growth (Romero-Vergel *et al*. 2022; Moreno-López *et al*. 2022). During each sampling visit, six cocoa trees were randomly selected and evaluated per farm, resulting in a total of 30 sampled trees over the course of the study in each farm. Trees were selected randomly at each visit to maximize spatial coverage within the plantations, and consequently different trees were assessed throughout the sampling period. For each tree, the total number of pods and their developmental stage were recorded. Pods were classified into five age groups: A) Pods between 0–10 days old, B) Pods between 10–30 days old, C) Pods between 30–60 days old, D) Pods between 60–90 days old, E) Pods older than 90 days (Figure 2).

Disease incidence study

Disease incidence was analyzed using generalized linear mixed models (GLMM) with abinomial distribution (Madden and Ojiambo 2024; Lan *et al*. 2022) and a logit link function, considering as the response variable the number of diseased pods relative to the total number of pods evaluated per sampling unit. Fixed effects included disease type (black pod and frosty pod rot), pod developmental stage (treated as an ordered factor), and canopy stratum (lower, middle, and upper). To account for the hierarchical structure of the sampling design and the dependence among repeated observations (Ocampo-Ariza *et al*. 2025), random intercepts were included for trees nested within farms. Models were fitted by maximum likelihood using the lme4 package (Bates *et al*. 2015). Model adequacy and assumption compliance were evaluated through diagnostic procedures implemented

PRE-PROOF PUBLICATION
PRE-PROOF PUBLICATION JOURNAL OF PLANT PROTECTION RESEARCH

in the performance package including tests for overdispersion and multicollinearity. Estimated marginal means and their 95% confidence intervals were calculated on the response scale using the emmeans package (Lenth 2021). Based on these marginal estimates, graphs were generated which represented predicted incidence for each disease as a function of pod developmental stage and canopy stratum. These figures were constructed from model-predicted values and visualized using the ggplot2 package (Wickham 2016), allowing a clear epidemiological interpretation of the main effects and their interactions.

Disease severity study

Disease severity was visually evaluated as the percentage of pod surface affected using the scale proposed by Murrieta and Palma (2018). Because severity values were bounded between 0 and 1 and represented biologically meaningful stages of disease development, observations were grouped into five ordinal categories representing disease progression (Chiang and Book 2022): Healthy (0), slightly rotten (>0–0.40), moderately rotten (>0.40–0.70), highly rotten (>0.70–<1), and completely rotten (1). The effects of disease type, pod developmental stage, and canopy layer on disease severity were evaluated using cumulative link models (CLM) with a logit link function implemented in the ordinal package for R (Christensen 2018). Candidate models were compared using likelihood-ratio tests and information criteria (AIC and BIC). The final model included disease type, pod developmental stage, and canopy layer as fixed effects. Model explanatory power was assessed using Nagelkerke's pseudo-R^2 calculated with the performance package (Lüdecke *et al*. 2021), while odds ratios were derived from model coefficients to quantify the magnitude of the effects.

Area under the disease progress curve

The area under the disease progress curve (AUDPC) was calculated from severity values obtained in successive sampling events for each tree × disease combination using the classical trapezoidal method described by Campbell and Madden (2007). Severity was expressed as the proportion of affected pod tissue (values between 0 and 1), and observations were conducted at regular intervals of 45 days. AUDPC was analyzed as a continuous variable using linear mixed models (LMM), considering disease type as a fixed effect and farm and tree (trees nested within farms) as random effects to account for the hierarchical sampling structure. Because the AUDPC values showed substantial positive skewness and a large proportion of zero observations, a square-root

PRE-PROOF PUBLICATION
PRE-PROOF PUBLICATION JOURNAL OF PLANT PROTECTION RESEARCH

transformation was applied before fitting the mixed-effects models to improve adherence to the assumptions of normality and homoscedasticity. Models were fitted using restricted maximum likelihood (REML) with the lme4 package (Pavicic *et al*. 2023), and were tested using Type III analysis of variance with Satterthwaite's approximation for degrees of freedom as implemented in the lmerTest package. Variance components from the global mixed model were estimated to quantify the relative contribution of different sources of variation (farm, tree within farm, and residual error). Estimated marginal means and pairwise comparisons between diseases were obtained using the emmeans package. Nakagawa's marginal and conditional coefficients of determination (R^2) and the intraclass correlation coefficient (ICC) were also calculated to quantify the proportion of variation explained by the fixed effects and by the hierarchical structure of the model. Model assumptions were assessed through residual diagnostics using the check_model function from the performance package. Additionally, residual normality was evaluated using the check_normality function, and homogeneity of variance was assessed using check_heteroscedasticity. Figures were generated with ggplot2 (Wickham 2016) using the observed AUDPC values.

Horizontal distribution of black pod and frosty pod rot incidence among cocoa farms

Horizontal distribution of cocoa disease incidence was analyzed within a georeferenced spatial framework using an exploratory and inferential approach. Incidence was calculated as the proportion of diseased pods relative to the total number of pods evaluated per sampling unit. Data preparation and management were conducted using the tidyverse package. Farm, tree, canopy stratum, and disease were treated as categorical variables. Geographic coordinates corresponded to the centroid of each farm and were used to construct spatial objects at the inter-farm scale, as trees were randomly sampled and did not have individual georeferencing. Records with missing values or zero pod counts were excluded. Geospatial objects were created using the simple features (sf) package (Pebesma 2018), converting the tabular dataset into a simple feature object referenced to the WGS84 geographic coordinate system (EPSG:4326). To enable distance-based spatial analyses and metric interpretation, spatial data were projected into the Universal Transverse Mercator (UTM) coordinate reference system corresponding to central Colombia (EPSG:32618). Horizontal distribution maps were generated using ggplot2 (Wickham 2016), where sampling locations were represented as spatial points scaled proportionally to disease incidence and color-coded according to disease type. Faceted panels were used to visualize patterns by farm. Axis breaks

PRE-PROOF PUBLICATION
PRE-PROOF PUBLICATION JOURNAL OF PLANT PROTECTION RESEARCH

were simplified to improve figure readability while preserving spatial resolution. The spatial location of disease observations was further explored using kernel density mapping (Hampf *et al*. 2021) through two-dimensional density estimation implemented in ggplot2 (Wickham 2016), and visualized by disease and farm. These maps were used solely as an exploratory visualization of the spatial distribution of disease observations Global spatial autocorrelation was evaluated separately for each disease using Moran's I index (Chen 2021) implemented with the spdep package. Spatial neighborhood relationships were defined based on k-nearest neighbors (k = 3), and row-standardized spatial weights were calculated to account for unequal connectivity among sampling points. Moran's I statistics and their associated significance tests were used to assess whether disease incidence exhibited evidence of spatial autocorrelation among sampling units represented by the centroids of the sampled farms.

Temporal effects of microclimatic variables on black pod and frosty pod rot incidence

The temporal distribution of black pod and frosty pod rot incidence was evaluated using generalized linear mixed models (GLMM) with a binomial distribution and logit link function implemented with the lme4 package (Barro *et al*. 2021). The response variable was specified as a binomial vector composed of the number of diseased pods and the number of healthy pods per observation unit. Analyses were conducted separately for each disease in order to evaluate differences in epidemiological responses to climatic variables. Fixed effects included temperature and relative humidity recorded during each sampling visit, using an AZ® data logger installed in the middle canopy layer of each evaluated tree. Both climatic variables had been previously centered and scaled to facilitate model convergence and allow comparison of effect sizes. To account for the hierarchical structure of the sampling design and the spatial dependence of the data, random intercepts were included for trees nested within farms. Models were fitted by maximum likelihood using the bobyqa optimizer. Model adequacy was evaluated through diagnostics for overdispersion and collinearity using the performance package. The significance of fixed effects was assessed using likelihood ratio tests. Adjusted marginal means of disease incidence were estimated for representative temperature values (−1, 0, and +1 standard deviation from the mean) using the emmeans package and expressed as probabilities with 95% confidence intervals.

PRE-PROOF PUBLICATION

PRE-PROOF PUBLICATION JOURNAL OF PLANT PROTECTION RESEARCH

Statistical analysis

All statistical analyses were conducted in R (version 4.5.2) using RStudio as the integrated development environment. The lme4, lmerTest, and ordinal packages were used for mixed-model fitting and cumulative link models; performance for model diagnostics and assumption checking, coefficients of determination (R^2), intraclass correlation coefficients (ICC), and pseudo-R^2 statistics; emmeans for estimation of marginal means; and tidyverse for data preprocessing, transformation, and visualization. Spatial analyses were conducted using the sf package for creating and handling spatial objects, enabling georeferenced analyses and spatial operations based on metric distances. Global spatial autocorrelation was assessed using the spdep package through the calculation of Moran's I index based on row-standardized spatial weights defined from k-nearest neighbors. Figures and graphical outputs were generated using the ggplot2 package (Wickham 2016).

Results

Morphological identification of microorganisms

Pods exhibiting different symptoms were collected from the three evaluated farms. The first group consisted of pods of different developmental stages showing necrotic lesions that led to mummification. Some pods also exhibited deformities commonly referred to as "humps." Visible signs of the pathogen were observed, including abundant white sporulation covering the affected areas (Figure 3A and 3B). When disease has progressed, pods become mummified (Figure 3C). These symptoms are consistent with frosty pod rot (Bailey *et al*. 2018; Pérez 2018) and microscopic examinations confirmed the presence of sporophores of *Moniliophthora* sp. (Figure 3D) in mummified pods showing visible pathogen signs. In pods exhibiting deformities, only fungal mycelium was observed. No symptoms associated with *Moniliophthora perniciosa* (Stahel) Aime & Phillips-Mora, such as witches' broom and the formation of strawberry-like or cherimoya-like pods (da Silva *et al*. 2022; Meraz-Pérez *et al*. 2021), were observed throughout the evaluation period on any of the farms surveyed.

The second group of pods exhibited necrotic lesions with well-defined margins, commonly referred to as "chocolate spot," as well as soft rots (Figure 3E). These symptoms were consistent with black pod disease. Microscopic observations confirmed the presence of coenocytic hyphae, sporangia, and chlamydospores characteristic of the genus *Phytophthora* (Figure 3F). It is important to note that several *Phytophthora* species have been reported as etiological agents of black pod disease in

PRE-PROOF PUBLICATION

PRE-PROOF PUBLICATION JOURNAL OF PLANT PROTECTION RESEARCH

Colombia, with *Phytophthora palmivora* being the most prevalent species (Rodríguez-Polanco *et al*. 2020).

Incidence of black pod and frosty pod rot during pod development

Predicted disease incidence showed notable variation between diseases and pod developmental stages (Table 1, Fig. 4). Black pod exhibited consistently low incidence across all pod age classes, with the lowest value observed at stage D (pods 60–90 days old) at 1.75% (95% confidence interval [CI]: 1.04–2.94) and the highest value in pods older than 90 days (stage E) at 5.45% (3.43–8.55). In contrast, frosty pod rot showed substantially higher incidence across all developmental stages, with the lowest value observed at stage D at 10.82% (6.96–16.44) and the highest value reaching 28.18% (20.13–37.93) at stage E.

Incidence of black pod and frosty pod rot by canopy stratum

Predicted disease incidence differed between diseases and canopy strata (Table 2, Fig. 5). Black pod exhibited low incidence across all canopy strata, with the lowest values observed in the lower stratum and increasing toward the middle and upper strata (1.53–3.92%). In contrast, frosty pod rot showed higher incidence values across all canopy strata, with the highest incidence occurring in the upper canopy layer (25.08%).

The GLMM with binomial distribution showed adequate fit (AIC = 1784.2; log-likelihood = −879.1). No overdispersion was detected (Pearson χ^2/df = 1.37; DHARMa dispersion test: p = 0.10), and zero-inflation was absent (ratio = 1.05, p = 0.154). Residual diagnostics based on 1000 DHARMa simulations revealed no significant outliers (bootstrap test: p = 0.10) and no temporal autocorrelation between visits (Durbin-Watson = 2.35, p = 0.665). Fixed effects explained 51.5% of variance (marginal R^2 = 0.515), with the full model accounting for 60.5% (conditional R^2 = 0.605; Nakagawa & Schielzeth 2013). The intraclass correlation coefficient (ICC = 0.185) confirmed substantial clustering by farm, tree, and visit, justifying the mixed-effects structure. The disease × canopy layer interaction was statistically significant ($\chi^2(2)$ = 6.73, p = 0.035), indicating that the effect of canopy position on disease incidence differed between black pod and frosty pod rot.

PRE-PROOF PUBLICATION

PRE-PROOF PUBLICATION JOURNAL OF PLANT PROTECTION RESEARCH

Severity of black pod and frosty pod rot during pod developmental stages

Overall, frosty pod rot exhibited substantially higher severity than black pod disease throughout the study, indicating a greater capacity to colonize and damage cacao fruits once infection was established.

Pod developmental stage strongly influenced disease severity (Table 3, Fig 6). Black pod severity remained low during stages A–D, ranging from 0.37% to 1.68%, and increased only in the most advanced developmental stage (E), where severity reached 5.30% (95% CI: 3.36–7.25). In contrast, frosty pod rot displayed considerably higher severity throughout fruit development, varying from 6.66% to 17.90%. The highest values were recorded in stage E (17.90%; 95% CI: 14.30–21.50), followed by stage B (13.20%; 95% CI: 10.80–15.50). Confidence intervals for frosty pod rot were consistently wider than those observed for black pod disease, reflecting greater variability between fruits. Despite this variability, the intervals of both diseases showed minimal overlap across developmental stages, indicating clear epidemiological differences in disease expression.

Severity of black pod and frosty pod rot across canopy strata

Disease severity also varied according to canopy position (Table 4, Fig 7). For black pod disease, severity increased progressively from the lower canopy (0.75%; 95% CI: 0.29–1.20) to the upper canopy (2.57%; 95% CI: 1.60–3.53). A similar but more pronounced pattern was observed for frosty pod rot, whose severity increased from 8.49% (95% CI: 6.70–10.30) in the lower canopy to 15.80% (95% CI: 13.50–18.20) in the upper canopy. The limited overlap among confidence intervals suggests that canopy position contributed substantially to disease development, particularly for frosty pod rot.

The cumulative link model converged successfully and yielded stable parameter estimates (maximum gradient = 7.28×10^{-8}; Hessian condition number = 1.3×10^{3}). Among the candidate models, the final model including disease type, pod developmental stage, and canopy layer provided the best fit (AIC = 3620.3, BIC = 3693.1, log-likelihood = −1799.2). Likelihood-ratio tests indicated that the inclusion of canopy layer and pod developmental stage significantly improved model performance ($p < 0.001$). The model explained 12.7% of the variation in severity classes (Nagelkerke's pseudo-$R^2 = 0.127$), supporting the adequacy of the ordinal framework for describing disease severity patterns in cacao fruits.

Disease type was the strongest predictor of severity class. Fruits affected by frosty pod rot

PRE-PROOF PUBLICATION

PRE-PROOF PUBLICATION JOURNAL OF PLANT PROTECTION RESEARCH

exhibited 5.91-fold greater probability of belonging to a higher severity category than fruits affected by black pod disease (OR = 5.91, $p < 0.001$). Likewise, fruits located in the upper canopy exhibited 2.21-fold greater probability of developing higher severity classes than fruits located in the lower canopy (OR = 2.21, $p < 0.001$). Pod developmental stage also significantly influenced severity class assignment, indicating that disease severity varied according to fruit maturity.

Area under the disease progress curve (AUDPC)

The adjusted mean AUDPC values were higher for frosty pod rot (14.0 ± 13.4 SD) than for black pod (7.0 ± 12.4 SD) (Table 5), indicating greater cumulative disease progression for frosty pod rot during the evaluation period. For both diseases, numerous trees exhibited low or null AUDPC values, while a few individuals showed high values, revealing pronounced heterogeneity in epidemic development at the tree scale (Fig. 8). The linear mixed-effects model fitted to square-root-transformed AUDPC values confirmed a significant effect of disease type on disease progress ($F = 5.27$, $df = 1,17$, $p = 0.0347$). Estimated marginal means were higher for frosty pod rot than for black pod disease, indicating a significantly greater accumulation of disease severity over time. Variance partitioning revealed that 19.0% of the total variation was attributable to differences between farms, 20.3% to differences between trees within farms, and 60.7% to residual variation (Table 6). Accordingly, the intraclass correlation coefficient (ICC = 0.393) indicated that nearly 40% of the total variability in AUDPC was associated with the hierarchical sampling structure, highlighting the importance of spatial heterogeneity in disease development.

Spatial distribution and hierarchical structure of black pod and frosty pod rot incidence

The incidence of black pod and frosty pod rot in cocoa exhibited variation between farms and canopy strata. The horizontal distribution map (Figure 9) showed differences in disease incidence between the three farms evaluated; however, no consistent spatial gradients were evident at the inter-farm scale represented by the farm centroids used in this study. In addition, Figure 10 illustrates the spatial location of disease observations used for the exploratory kernel analyses. These maps provide a descriptive visualization of disease observations across farms and disease types and should not be interpreted as evidence of spatial aggregation or disease hotspots, as the analyses were based on farm centroids rather than individual tree coordinates.

Global spatial autocorrelation analyses (Table 7) did not detect significant spatial

PRE-PROOF PUBLICATION
PRE-PROOF PUBLICATION JOURNAL OF PLANT PROTECTION RESEARCH

autocorrelation for either disease (black pod: $I \approx 0$, $p = 0.468$; frosty pod rot: $I = 0.011$, $p = 0.243$), indicating that disease incidence did not exhibit detectable spatial structure at the inter-farm scale represented by the farm centroids used in this study. Furthermore, variance components determined from the binomial generalized linear mixed model showed that most of the explained variability was associated with differences between trees within farms (62.4%), whereas farm-level variation accounted for only 4.4% of the total variance (Table 8). In addition, disease incidence increased significantly with canopy height and was consistently higher for frosty pod rot, particularly in the upper canopy layer, suggesting that the micro-environment and a vertical position of pods play a more important role in the epidemiological dynamics of these diseases than spatial differences between farms.

Temporal effects of microclimatic variables on the incidence of black pod and frosty pod rot

Temporal patterns of disease incidence differed markedly between black pod and frosty pod rot. In the case of black pod, baseline incidence was low ($\beta = -3.742 \pm 0.290$ SE, $p < 0.001$), and neither temperature ($\beta = 0.197 \pm 0.197$ SE, $p = 0.316$) nor relative humidity ($\beta = 0.001 \pm 0.224$ SE, $p = 0.995$) showed significant effects on temporal variation in disease incidence. Most of the variability attributable to the random effects was concentrated at the tree level (variance = 0.831), whereas the contribution of farm-level variation was limited (variance = 0.034), indicating strong local heterogeneity and a limited spatial structure at the farm scale (Table 9). In contrast, frosty pod rot exhibited a higher baseline incidence ($\beta = -1.608 \pm 0.190$ SE, $p < 0.001$) and showed significant negative associations with both temperature ($\beta = -0.208 \pm 0.086$ SE, $p = 0.016$) and relative humidity ($\beta = -0.429 \pm 0.088$ SE, $p < 0.001$). These results indicated a negative association between frosty pod rot incidence and the temperature and relative humidity values recorded during the evaluation period. Variance components revealed moderate variability at both the tree level (variance = 0.158) and the farm level (variance = 0.071), suggesting that the temporal dynamics of the disease were influenced by factors operating at both local and broader spatial scales (Table 10).

Model diagnostics supported the adequacy of the binomial GLMMs. No evidence of overdispersion was detected for either black pod disease (dispersion ratio = 1.55, $p = 0.224$) or frosty pod rot (dispersion ratio = 1.57, $p = 0.064$), and multicollinearity among predictors was low (VIF < 2). Marginal R^2 values were low (0.015–0.050), indicating that the evaluated microclimatic variables explained only a small fraction of the variation in disease incidence. In contrast, higher conditional

PRE-PROOF PUBLICATION
PRE-PROOF PUBLICATION JOURNAL OF PLANT PROTECTION RESEARCH

R^2 values (0.164–0.351) and the corresponding intraclass correlation coefficients (ICC = 0.120–0.341) highlighted the importance of the hierarchical farm–tree structure in shaping disease incidence patterns. Overall, these diagnostics support the suitability of the fitted GLMMs for assessing temporal variation in disease incidence.

Discussion

The objective of this study was to determine the epidemiological patterns of frosty pod rot and black pod, two of the most limiting diseases affecting production in Viotá, Cundinamarca. A limitation of this study was that pathogen identification was conducted only to the genus level, and therefore the specific species involved in disease development were not determined. This may be particularly relevant for black pod disease, which can be caused by different *Phytophthora* species in Colombia, although the predominant species is *P. palmivora* (Ramírez-Martínez *et al*. 2026). To support disease diagnosis, symptomatic pods were subjected to morphological examination and pathogenicity tests, confirming the presence of microorganisms consistent with *Moniliophthora* sp. and *Phytophthora* spp. as the causal agents of the observed diseases. Furthermore, disease monitoring was based on symptom expression on pods, reflecting the approach commonly used by farmers for phytosanitary surveillance and management decisions. Consequently, the epidemiological patterns described here remain directly relevant for disease monitoring and management in cocoa production systems, The incidence and severity of black pod and frosty pod rot showed significant variation with fruit age. For black pod, pods at stage E (older than 90 days) showed the highest level of infection. Rodríguez-Polanco *et al*. (2020a) reported that the stage of greatest susceptibility to black pod in the CCN51 clone occurs between two and four months of pod development and later stages. For frosty pod rot, pods aged 60 days and older (groups D and E) exhibited the highest incidence and severity. Bailey *et al*. (2018) indicated that the later stages of cocoa fruit development allow *M. roreri* to reach both the biotrophic and necrotrophic phases during pathogenesis. This pathogen is hemibiotrophic with a prolonged biotrophic phase (45–90 days), which may be reflected in the severity levels observed in this study.

Among the different canopy strata, the upper canopy exhibited the highest incidence and severity for both diseases. The absence of significant differences between the lower and middle strata suggests that disease pressure was not uniformly distributed throughout the canopy but rather concentrated in zones with more favorable environmental conditions for pathogen

PRE-PROOF PUBLICATION
PRE-PROOF PUBLICATION JOURNAL OF PLANT PROTECTION RESEARCH

establishment. Cultural management practices may also influence these patterns. Due to tree height and the limited technological management typical of many cocoa plantations (Hernández-Núñez *et al*. 2025), pruning in the upper canopy is often less uniform, resulting in denser foliage and the formation of a microclimate that favors pathogen survival and dispersal (Jaimes *et al*. 2022; Jaimes *et al*. 2016).

A vertical position also constitutes an independent risk factor for disease incidence. It is likely that canopy effects interact with pod age and pathogen type. Younger and intermediate-stage pods located in the upper canopy may be more frequently exposed to primary and secondary inoculum of *Phytophthora* spp. and *M. roreri*, whereas more mature pods in the same stratum may accumulate longer exposure periods under favorable environmental conditions. Because the upper canopy is more exposed to rainfall, free water retention on pod surfaces and increased inoculum deposition through splash dispersal may create favorable conditions for *P. palmivora* and *M. roreri* (Perrine-Walker 2020; Bailey *et al*. 2018). Gramacho *et al*. (2018) reported that sporophores of *M. roreri* are dispersed downward by wind, which could explain the higher incidence and severity of frosty pod rot in the upper canopy. Contrary to the findings of this study, Opoku *et al.* (2007) reported higher pod rot rates at the base of cocoa trees than in the canopy. In cocoa trees affected by *Phytophthora megakarya*, pod position within the canopy had a significant effect on black pod disease incidence; however, this effect was less pronounced when *P. palmivora* was the causal pathogen. Several factors may have accounted for these differences, including cultural management practices, such as pruning regimes and frequency, as well as the clones cultivated in the Tequendama region.

In very few trees, pods exhibiting symptoms of both diseases were observed; however, in most cases, infections occurred independently. Although previous studies have evaluated incidence and severity of black pod rot and frosty pod rot simultaneously within the same cocoa plants, but they did not assess concurrent coinfection (Lopez Torres *et al*. 2025; Anzules *et al*. 2022). The presented results did not provide evidence that competition for space or nutrients influenced the higher incidence and severity of frosty pod rot compared with black pod disease. Therefore, the differences observed between diseases were more likely associated with their distinct epidemiological characteristics and responses to environmental conditions than with direct interactions between the pathogens.

Global spatial autocorrelation analyses did not detect significant spatial autocorrelation in the

PRE-PROOF PUBLICATION
PRE-PROOF PUBLICATION JOURNAL OF PLANT PROTECTION RESEARCH

incidence of either black pod disease or frosty pod rot, indicating that disease incidence did not exhibit a detectable spatial structure at the inter-farm scale represented in this study. Kernel density maps identified areas with a higher apparent concentration of disease observations; however, these patterns should be interpreted cautiously because they largely reflected the hierarchical sampling structure rather than formal evidence of pathogen aggregation. Since spatial analyses were based on farm centroids rather than individually georeferenced trees, the absence of significant spatial autocorrelation should not be interpreted as evidence of completely random disease distribution. Instead, the results were consistent with disease dynamics being influenced primarily by local-scale factors and vertical canopy processes rather than by broad horizontal spatial gradients among farms. Additional studies incorporating georeferenced tree-level data and more extensive geostatistical analyses would be necessary to evaluate fine-scale spatial aggregation patterns. From an epidemiological perspective, these findings suggest that disease management may benefit more from tree-level interventions, such as the timely removal of infected pods and canopy pruning (Adeniran *et al*. 2024; Almestar-Montenegro *et al*. 2024; Ndoumbe-Nkeng *et al*. 2004).

During the study period, mean temperatures and relative humidity across the three farms were 29.15 ± 2.14°C and 61.76 ± 7.78%, respectively. Although the recorded temperatures were generally within the range considered favorable for frosty pod rot development, relative humidity remained below values typically associated with severe epidemics. Previous studies have reported that frosty pod rot is favored by high relative humidity, the presence of free water on pod surfaces, and temperatures between 22 and 28°C (Sánchez *et al*. 2017). Likewise, Jiménez *et al*. (2022) and Leandro-Muñoz *et al*. (2017) reported that epidemic development of *M. roreri* is favored by relative humidity levels above 80% and prolonged periods of pod wetness. In contrast, the present study detected a negative association between frosty pod rot incidence and both temperature and relative humidity. This apparent discrepancy may reflect the relatively narrow range of environmental conditions observed during the evaluation period, as well as the fact that microclimatic measurements were recorded only during daytime sampling visits (08:00–12:00 h) and therefore may not have captured nocturnal humidity peaks or periods of pod wetness that are critical for infection. Despite frosty pod rot exhibiting higher incidence and severity than black pod disease, incidence values remained below 25%, suggesting that environmental conditions during the study period were only moderately favorable for epidemic development.

In contrast, no significant effects of temperature or relative humidity on black pod incidence were detected in the present study. This finding differed from the results reported by Fofana *et al*. (2025) in

PRE-PROOF PUBLICATION

PRE-PROOF PUBLICATION JOURNAL OF PLANT PROTECTION RESEARCH

Côte d'Ivoire, where black pod incidence was positively associated with relative humidity and rainfall and negatively associated with temperature. Such discrepancies may reflect differences in environmental conditions, pathogen populations, management practices, or the temporal resolution of climatic measurements among studies. Furthermore, the relatively low humidity levels recorded during the evaluation period may have limited the development of conditions conducive to severe black pod epidemics.

Other factors that may influence disease development—such as precipitation, wind, insects, rodents, bats, and human activity (Moura *et al*. 2025; Merga 2022; Delgado-Ospina *et al*. 2021; Jaimes *et al*. 2019; Ndoumbè-Nkeng *et al.* 2009; Dennis and Konam 1994)—were not considered in this study and should be included in future research to better understand epidemic dynamics. Additionally, comparisons between agroforestry systems and monoculture cocoa systems may provide further insight into disease epidemiology. In addition, the assessment of pathogen incidence and severity under field conditions has relied on laborious and subjective visual inspections, thereby constraining the responsiveness capacity to dynamic epidemiological processes. Nevertheless, the implementation of advanced digital tools—such as optimized deep learning architectures designed for automated plant tissue damage recognition—enables more agile, accurate, and large-scale spatiotemporal monitoring (Nyarko *et al*. 2024). The integration of such early digital diagnostics with classical epidemiological models would not only optimize the estimation of variables like disease incidence (percentage of diseased pods) and yield losses, but would also facilitate a deeper comprehension of the interactions between environmental drivers and inoculum dispersal. Consequently, this approach provided objective datasets for the design of more efficient and sustainable integrated pest management (IPM) strategies, mitigating reliance on massive chemical treatments and enhancing the selection of tolerant genotypes in breeding programs, an aspect that warrants consideration for future research.

Conclusions

This study provided an integrated epidemiological assessment of black pod and frosty pod rot in cocoa plantations in the Tequendama region of Colombia through the combined use of hierarchical mixed-effects models, ordinal regression models, geostatistical approaches, and spatial autocorrelation analysis. The results suggested that both diseases exhibit contrasting temporal dynamics and spatial patterns across canopy strata and sampling scales within the studied farms from

PRE-PROOF PUBLICATION
PRE-PROOF PUBLICATION JOURNAL OF PLANT PROTECTION RESEARCH

a temporal perspective. Disease-specific models revealed contrasting responses to climatic variables. Frosty pod rot incidence showed a significant negative association with temperature and relative humidity, suggesting strong sensitivity to environmental conditions during the evaluation period. In contrast, black pod incidence did not show a significant climatic response within the observed environmental range. These findings suggest that the temporal dynamics of frosty pod rot were more closely coupled to microclimatic fluctuations, whereas black pod dynamics may be more strongly influenced by local inoculum availability and host susceptibility.

Overall, this study highlighted the value of combining hierarchical statistical models with explicit spatial analytical tools to advance the understanding of disease dynamics in perennial cropping systems. This approach may provide a useful methodological framework for designing precision disease management strategies and for future research on the interactions between climate, canopy structure, and inoculum dispersal in tropical agroecosystems.

Funding

This research was funded by the Ministry of Science, Technology and Innovation (MINCIENCIAS), University of Cundinamarca and National University of Colombia (Bogotá) through the call "802-2018 R&D Projects for Biological-Based Technological Development, Department of Cundinamarca".

Acknowledgments

The authors wish to thank Dr. Adriana González Almario (Faculty of Agricultural Sciences, Universidad Nacional de Colombia – Bogotá Campus) and Professor César Ariza Castillo (Faculty of Agricultural Sciences, Universidad de Cundinamarca) for their contributions to manuscript review and statistical analysis. The authors also want to thank the Bajo Tequendama Cocoa Growers Association (ASCABATE) for allowing field sampling on their cocoa farms and for their contributions to manuscript review and statistical analysis. The authors also thank the Bajo Tequendama Cocoa Growers Association (ASCABATE) for allowing field sampling on their cocoa farms.

PRE-PROOF PUBLICATION

PRE-PROOF PUBLICATION JOURNAL OF PLANT PROTECTION RESEARCH

References

Abad Z.G., Burgess T.I., Redford A.J., Bienapfl J.C., Srivastava S., Mathew R., Jennings K. 2023. IDphy: An international online resource for molecular and morphological identification of Phytophthora based on type specimens. Plant Disease 107(4): 987–998. DOI: https://doi.org/10.1094/PDIS-02-22-0448-FE

Adeniran A.O., Onanaye A.S., Adeleke O.J. 2024. Optimal control of cocoa black pod disease: a multi-pronged approach. Franklin Open 7: 100100. DOI: https://doi.org/10.1016/j.fraope.2024.100100

Almestar-Montenegro J., Leiva-Espinoza S., Borjas-Ventura R., Valderrama-Palacios D., León-Rojas F., Castro-Cepero V., Alvarado-Huamán L., Julca-Otiniano A. 2024. Efecto de la poda y la remoción de frutos sobre las enfermedades de la mazorca de cacao en Copallín, Amazonas, Perú. Idesia (Arica) 42 (4): 69–77. DOI: https://doi.org/10.4067/S0718-34292024000400069

Alsultan W., Yun W.M., Ahmad Z.A.M., Vadamalai G., Khairulmazmi A., Al-Sadi A.M., Rashed O., Nasehi A., Al-Tawaha A.R. 2022. Morphological, pathogenic, and molecular characterization of *Phytophthora palmivora* isolates causing black pod disease on cocoa in Peninsular Malaysia. *International Journal of Food Science and Agriculture* 6(2): 135–148. DOI: https://doi.org/10.26855/ijfsa.2022.06.002

Alves da Silva N.J., Menezes Reis S.P., Diorato V.S., Rocha J.S.A., Barbosa C.S., Ciampi-Guillardi M., Patrocínio N.G.R.B., Niella G.R., Solis K., Peñaherrera S., Manco M.J.S., Teixeira G.A., Arévalo-Gardini E., Gramacho K.P. 2022. A molecular diagnostic for *Moniliophthora perniciosa*, the causal agent of witches' broom disease of cacao, that differentiates it from its sister taxon *Moniliophthora roreri*. *Crop Protection* 158: 106003. https://doi.org/10.1016/j.cropro.2022.106003

Anzules-Toala V., Pazmiño-Bonilla E., Alvarado-Huamán L., Borjas-Ventura R., Castro-Cepero V., Julca-Otiniano A. 2021. Control of cacao (*Theobroma cacao*) diseases in Santo Domingo de los Tsachilas, Ecuador. *Agronomía Mesoamericana* 33(1): 45939. DOI: https://doi.org/10.15517/am.v33i1.45939

Bailey B.A., Evans H.C., Phillips-Mora W., Ali S.S., Meinhardt L.W. 2018. *Moniliophthora roreri*, causal agent of cacao frosty pod rot. Molecular Plant Pathology 19 (7): 1580–1594. DOI: https://doi.org/10.1111/mpp.12648

PRE-PROOF PUBLICATION

PRE-PROOF PUBLICATION JOURNAL OF PLANT PROTECTION RESEARCH

Bailey B.A., Meinhardt L.W. (eds.). 2016. Cacao Diseases: A History of Old Enemies and New Encounters. Springer, Cham, Switzerland, 633 pp. DOI: https://doi.org/10.1007/978-3-319-24789-2

Barro M., Kassankogno A.I., Wonni I., Séréme D., Somda I., Kabore H.K., Bena G., Brugidou C., Tharreau D., Tollenaar C. 2021. Spatiotemporal survey of multiple rice diseases in irrigated areas compared to rainfed lowlands in the Western Burkina Faso. *Plant Disease* 105: 3889–3899. https://doi.org/10.1094/PDIS-03-21-0579-RE

Bates D., Mächler M., Bolker B., Walker S. 2015. Fitting linear mixed-effects models using lme4. Journal of Statistical Software 67(1): 1–48. DOI: https://doi.org/10.18637/jss.v067.i01

Charry A., Perea C., Ramírez K., Zambrano G., Yovera F., Santos A., Pulleman M. 2025. The bittersweet economics of different cacao production systems in Colombia, Ecuador and Peru. Agricultural Systems 224: 104235. DOI: https://doi.org/10.1016/j.agsy.2024.104235

Chen Y. 2021. An analytical process of spatial autocorrelation functions based on Moran's index. PLoS ONE 16 (4): e0249589. DOI: https://doi.org/10.1371/journal.pone.0249589

Chiang K.S., Bock C.H. 2022. Understanding the ramifications of quantitative ordinal scales on accuracy of estimates of disease severity and data analysis in plant pathology. Tropical Plant Pathology 47(1): 58–73. DOI: https://doi.org/10.1007/s40858-021-00446-0

Christensen R.H.B. 2018. Cumulative Link Models for Ordinal Regression with the R Package ordinal. Technical report, R package ordinal. Available at: https://cran.r-project.org/web/packages/ordinal/vignettes/clm_article.pdf

Correa A.J., Castro M.S., Coy J. 2014. Estado de la moniliasis del cacao causada por *Moniliophthora roreri* en Colombia. Acta Agronómica 63 (4): 388–399. DOI: https://doi.org/10.15446/acag.v63n4.42747

Delgado-Ospina J., Molina-Hernández J.B., Chaves-López C., Romanazzi G., Paparella A. 2021. The role of fungi in the cocoa production chain and the challenge of climate change. Journal of Fungi 7 (3): 202. DOI: https://doi.org/10.3390/jof7030202

Federación Nacional de Cacaoteros (FEDECACAO). 2025. Colombia reportó en 2024 producción histórica de cacao. [Online]. Available from: https://www.fedecacao.com.co/post/colombia-reportó-en-2024-producción-histórica-de-cacao [accessed 14 June 2026].

Fofana B., Patrick D.J., Miyasi B.W., Zouzou M., Daouda K. 2025. Influence of climatic parameters on the incidence of black pod rot of cocoa trees in Côte d'Ivoire. Journal of Experimental

PRE-PROOF PUBLICATION

PRE-PROOF PUBLICATION JOURNAL OF PLANT PROTECTION RESEARCH

Agriculture International 47 (1): 161–170. DOI: https://doi.org/10.9734/JEAI/2025/v47i13214

Gobernación de Cundinamarca. 2025. Cundinamarca siembra futuro con cacao: más de 100000 nuevas plántulas y proyectos para 3500 familias rurales. [Online]. Available from: https://www.cundinamarca.gov.co/dependencias/secagrocampesinado/noticias/cundinamarca-siembra-futuro-con-cacao-mas-de-100000-nuevas-plantulas-y-proyectos-para-3500-familias-rurales [accessed 14 June 2026].

Gramacho K.P., Albuquerque P., Novais C.B., Lopes U.V., Sobrinho C.M. 2018. Moniliophthora roreri (Cif & Par.) (Agaricales: Marasmiaceae). pp. 257–269. In: "Priorização de pragas quarentenárias ausentes no Brasil" (E.G. Fidelis, T.R. Lohmann, M.L. da Silva, P. Parizzi, F.F.L. Barbosa, eds.). Embrapa, Brasília, DF, Brazil.

Hampf A.C., Nendel C., Strey S., Strey R. 2021. Biotic yield losses in the Southern Amazon, Brazil: making use of smartphone-assisted plant disease diagnosis data. Frontiers in Plant Science 12: 621168. DOI: https://doi.org/10.3389/fpls.2021.621168

Hernández-Núñez H.E., Suárez J.C., Andrade H.J., Bernal Núñez A.P., Gutiérrez D.R., Gutiérrez G.A., Gutiérrez-Montes I., Méndez V.E., Casanoves F. 2025. Agronomic performance of cocoa production type systems in Colombia. *PLOS One* 20 (12): e0337624. DOI: https://doi.org/10.1371/journal.pone.0337624

Hipólito-Romero E., Cocoletzi-Vásquez E., Ramos-Prado J.M., Espinoza C., Torres-de la Cruz M., Ricaño-Rodríguez J. 2020. Breve aproximación a la naturaleza genómica de *Moniliophthora roreri* CPMRT01 aislado de cacao en Tabasco, México. Biotecnia 22 (2): 39–49. DOI: https://doi.org/10.18633/biotecnia.v22i2.1244

Jaimes-Suárez Y.Y., Carvajal-Rivera A.S., Galvis-Neira D.A., Carvalho F.E., Rojas-Molina J. 2022. Cacao agroforestry systems beyond the stigmas: biotic and abiotic stress incidence impact. Frontiers in Plant Science 13: 921469. DOI: https://doi.org/10.3389/fpls.2022.921469

Jaimes Y.Y., Ribeyre F., Gonzalez C., Rojas J., Furtado E.L., Cilas C. 2019. Factors affecting the dynamics of frosty pod rot in the main cocoa areas of Santander state, Colombia. Plant Disease 103(7): 1665–1673. DOI: https://doi.org/10.1094/PDIS-10-18-1761-RE

Jaimes Y.Y., Gonzalez C., Rojas J., Cornejo O.E., Mideros M.F., Restrepo S., Cilas C., Furtado E.L. 2016. Geographic differentiation and population genetic structure of Moniliophthora roreri in the principal cocoa production areas in Colombia. Plant Disease 100(8): 1548–1558. DOI:

PRE-PROOF PUBLICATION

PRE-PROOF PUBLICATION JOURNAL OF PLANT PROTECTION RESEARCH

https://doi.org/10.1094/PDIS-12-15-1498-RE

Jibat M., Alo S. 2023. Integrated management of black pod (*Phytophthora palmivora*) disease of cocoa through fungicides and cultural practices in Southwestern Ethiopia. International Journal on Food, Agriculture and Natural Resources 4 (3): 43–45. DOI: https://doi.org/10.46676/ij-fanres.v4i3.150

Jiménez D.L., Alvarez J.C., Mosquera S. 2022. Frosty pod rot: a major threat to cacao plantations on the move. Tropical Plant Pathology 47 (2): 187–200. DOI: https://doi.org/10.1007/s40858-021-00472-y

Kongor J.E., Owusu M., Oduro-Yeboah C. 2024. Cocoa production in the 2020s: challenges and solutions. CABI Agriculture and Bioscience 5: 102. DOI: https://doi.org/10.1186/s43170-024-00310-6

Lan Y.H., Shaw D.C., Lee E.H., Beedlow P.A. 2022. Distribution of a foliage disease fungus within canopies of mature Douglas-fir in Western Oregon. Frontiers in Forests and Global Change 5: 743039. DOI: https://doi.org/10.3389/ffgc.2022.743039

Leandro-Munoz M.E., Tixier P., Germon A., Rakotobe V., Phillips-Mora W., Maximova S., Avelino J. 2017. Effects of microclimatic variables on the symptoms and signs onset of *Moniliophthora roreri*, causal agent of *Moniliophthora* pod rot in cacao. PLoS ONE 12 (10): e0184638. DOI: https://doi.org/10.1371/journal.pone.0184638

Lenth R.V. 2021. emmeans: Estimated Marginal Means, aka Least-Squares Means. R package version 1.6.0. Available from: https://CRAN.R-project.org/package=emmeans

López-Torres M.E., Ramírez-Argueta O.A., Dubon Dubon A., Diaz Matute F.J. 2025. Selecting cacao clones with high productivity potential and tolerance to black pod rot (*Phytophthora* sp.) and frosty pod rot (*Moniliophthora roreri*). Journal of Plant Protection Research 65: 535–547. DOI: https://doi.org/10.24425/jppr.2025.156888

Lüdecke D., Ben-Shachar M.S., Patil I., Waggoner P., Makowski D. 2021. performance: An R package for assessment, comparison and testing of statistical models. Journal of Open Source Software 6 (60). DOI: https://doi.org/10.21105/joss.03139

Madden L.V., Hughes G., van den Bosch F. 2007. The Study of Plant Disease Epidemics. 2nd ed. APS Press, St. Paul, Minnesota, USA, 421 pp. DOI: https://doi.org/10.1094/9780890545058

Madden L.V., Ojiambo P.S. 2024. The value of generalized linear mixed models for data analysis in the plant sciences. Frontiers in Horticulture 3: 1423462. DOI:

PRE-PROOF PUBLICATION

PRE-PROOF PUBLICATION JOURNAL OF PLANT PROTECTION RESEARCH

https://doi.org/10.3389/fhort.2024.1423462

Mejia-Cervantes L.E., Mendoza-Thompson J.U. 2026. Underestimation of the economic impact of moniliasis and witches' broom on *Theobroma cacao* L. Frontiers in Sustainable Food Systems 10: 1726828. DOI: https://doi.org/10.3389/fsufs.2026.1726828

Meraz-Pérez I.M., Carvalho M.R., Sena K.F., Soares Y.J.B., Estrela Junior A.S., Lopes U.V., dos Santos Filho L.P., Araújo S.A., Soares V.L.F., Pirovani C.P., Gramacho K.P. 2021. The *Moniliophthora perniciosa*–cacao pod pathosystem: Structural and activated defense strategies against disease establishment. *Physiological and Molecular Plant Pathology* 115: 101656. DOI: https://doi.org/10.1016/j.pmpp.2021.101656

Merga J. 2022. Epidemiology and management strategies of cocoa black pod (*Phytophthora* spp.). Plant Pathology & Quarantine 12 (1): 34–39. DOI: https://doi.org/10.5943/ppq/12/1/2

Mora F.D., Fiallos F.R. 2012. *Moniliophthora roreri* Evans et al. in the crop of cacao. Scientia Agropecuaria 3 (3): 249–258. DOI: https://doi.org/10.17268/sci.agropecu.2012.03.06

Moreno-Lopez J.P., Banda-Sánchez L.D.C., Gil-Clavijo A.I., Méndez-Pineda D.O., Márquez-Niño F.G. 2022. Aspectos de la investigación del cacao en municipios de la zona del Tequendama. Editorial Universidad de Cundinamarca. Fusagasugá, Colombia, 80 pp. DOI: https://doi.org/10.36436/9786287621190

Moura V.B., Pantoja L.P., Cavalcante Filho E.H., Haber R.A., Leandro-Silva V., Costa D.L.P., Júnior M.A., Franco T.M., Nery M.K.M., Rua M.L., de Souza P.J.O.P. 2025. Current bioclimatic suitability and climate change impacts on the risk of cacao moniliasis invasion in Pará. *Ecological Modelling* 505: 111106. DOI: https://doi.org/10.1016/j.ecolmodel.2025.111106

Murrieta E., Palma H. 2018. Manual de buenas prácticas de cosecha y postcosecha de cacao a nivel de productor. USAID–Alianza Cacao Perú, Lima, Perú, 43 pp. Available from: https://pdf.usaid.gov/pdf_docs/PA00XDCP.pdf [accessed 14 June 2026].

Ndoumbè-Nkeng M., Efombagn M.I.B., Nyassé S., Nyemb E., Sache I., Cilas C. 2009. Relationships between cocoa *Phytophthora* pod rot disease and climatic variables in Cameroon. Canadian Journal of Plant Pathology 31 (3): 309–320. DOI: https://doi.org/10.1080/07060660909507605

Ndoumbe-Nkeng M., Cilas C., Nyemb E., Nyassé S., Bieysse D., Flori A., Sache I. 2004. Impact of removing diseased pods on cocoa black pod caused by *Phytophthora megakarya* and on

PRE-PROOF PUBLICATION

PRE-PROOF PUBLICATION JOURNAL OF PLANT PROTECTION RESEARCH

cocoa production in Cameroon. Crop Protection 23 (5): 415–424. DOI: https://doi.org/10.1016/j.cropro.2003.09.010

Nyarko B.N.E., Wu W.B., Zhou J.Z., Mohd M.M.J. 2024. Improved YOLOv5m model based on Swin Transformer, K-means++, and Efficient Intersection over Union (EIoU) loss function for cocoa tree (Theobroma cacao) disease detection. Journal of Plant Protection Research 64 (3): 265–274. DOI: https://doi.org/10.24425/jppr.2024.151253

Opoku I.Y., Akrofi A.Y., Appiah A.A. 2007. Assessment of sanitation and fungicide application directed at cocoa tree trunks for the control of *Phytophthora* black pod infections in pods growing in the canopy. European Journal of Plant Pathology 117 (2): 167–175. DOI: https://doi.org/10.1007/s10658-006-9082-8

Pavicic M., Mouhu K., Hautsalo J., Jacobson D., Jalli M., Himanen K. 2023. Image-based time series analysis to establish differential disease progression for two *Fusarium* head blight pathogens in oat spikelets with variable resistance. Frontiers in Plant Science 14: 1126717. DOI: https://doi.org/10.3389/fpls.2023.1126717

Pebesma E. 2018. Simple features for R: standardized support for spatial vector data. The R Journal 10 (1): 439–446. DOI: https://doi.org/10.32614/RJ-2018-009

Perrine-Walker F. 2020. *Phytophthora palmivora*–cocoa interaction. Journal of Fungi 6 (3): 167. DOI: https://doi.org/10.3390/jof6030167

Ramírez-Martínez J., Cárdenas M., Duitama J., Duarte D., Gutiérrez Rodríguez E., Restrepo S. 2026. High genetic diversity of *Phytophthora palmivora* in Colombian cacao: Evidence against geographic barriers. Phytopathology. Published online: 15 Apr 2026. DOI: https://doi.org/10.1094/PHYTO-10-25-0351-R

Ramírez Martínez J., Cárdenas Toquica M., Guevara-Suarez M., Duarte D., Victorino Jimenez L.D., Argüello Bernal B.K., Gutiérrez Rodríguez E., Restrepo Restrepo S. 2021. Oomycete species associated with *Theobroma cacao* crops in Colombia. *Plant Pathology* 70 (7): 1695–1707. DOI: https://doi.org/10.1111/ppa.13410

Rodriguez-Medina C., Arana A.C., Sounigo O., Argout X., Alvarado G.A., Yockteng R. 2019. Cacao breeding in Colombia, past, present and future. Breeding Science 69 (3): 373–382. DOI: https://doi.org/10.1270/jsbbs.19011

Rodríguez-Polanco E., Alferes E.B., Fuquene P.A., Amaya J.D., Polanco L.A. 2020a. Manejo de la pudrición parda de la mazorca (Phytophthora palmivora) en cacao por aplicación conjunta

PRE-PROOF PUBLICATION

PRE-PROOF PUBLICATION JOURNAL OF PLANT PROTECTION RESEARCH

de prácticas culturales y químicas. Revista Facultad de Ciencias Básicas 16(1): 79–94. DOI: https://doi.org/10.18359/rfcb.4887

Rodríguez-Polanco E., Morales J.G., Muñoz-Agudelo M., Segura J.D., Carrero M.L. 2020b. Morphological, molecular and pathogenic characterization of Phytophthora palmivora isolates causing black pod rot of cacao in Colombia. Spanish Journal of Agricultural Research 18(2): e1003. DOI: https://doi.org/10.5424/sjar/2020182-15147

Rojas G. M., Benavides R.M., Mayorga G.D., Manjarres D. 2014. Línea base y componentes agroecológicos de un sistema productivo de cacao en el municipio de Medina, Cundinamarca. *Inventum* 9 (17): 16–22. DOI: https://doi.org/10.26620/uniminuto.inventum.9.17.2014.16-22

Romero-Vergel A.P., Camargo- Rodríguez A.V., Ramírez O.D., Arenas Velilla P.A., Gallego A.M. 2022. A crop modelling strategy to improve cacao quality and productivity. Plants 11 (2): 157. DOI: https://doi.org/10.3390/plants11020157

Tovar-León J.A., Silva-Cobos D.C., Mateus-Vargas L.N. 2023. Análisis de la cadena productiva de cacao en los contextos local y nacional de Colombia. *Ciencias Agropecuarias* 9 (1): 39–60. DOI: https://doi.org/10.36436/24223484.370

Vanegas J.I., Suárez J.C., Casanoves F., Phillips-Mora W. 2026. Performance of cacao clones resistant to frosty pod rot under agroforestry systems and full sun in the Colombian Amazon. Agroforestry Systems 100 (1): 13. DOI: https://doi.org/10.1007/s10457-025-01384-5

Villamizar-Gallardo R., Osma J.F., Ortíz-Rodríguez O.O. 2019. Regional evaluation of fungal pathogen incidence in Colombian cocoa crops. Agriculture 9 (3): 44. DOI: https://doi.org/10.3390/agriculture9030044

Wickham H. 2016. Data analysis. pp. 189–201. In: "ggplot2: Elegant Graphics for Data Analysis". Springer International Publishing, Cham, Switzerland. DOI: https://doi.org/10.1007/978-3-319-24277-4_9

PRE-PROOF PUBLICATION

PRE-PROOF PUBLICATION JOURNAL OF PLANT PROTECTION RESEARCH

Table 1. Estimated incidence of black pod and frosty pod rot according to pod age in cocoa.

Disease	Pod age	Estimated incidence % (95% CI)
Black pod	A	2.15 (1.31–3.50)
	B	3.47 (2.20–5.45)
	C	2.32 (1.40–3.81)
	D	1.75 (1.04–2.94)
	E	5.45 (3.43–8.55)
Frosty pod rot	A	13.02 (8.69–19.05)
	B	19.68 (13.83–27.22)
	C	13.91 (9.20–20.48)
	D	10.82 (6.96–16.44)
	E	28.18 (20.13–37.93)

Values represent the estimated disease incidence (%) with 95% confidence intervals (CI), obtained from a generalized linear mixed model (GLMM) with a binomial error distribution and logit link function. The model included disease type, pod age class, and canopy layer as fixed effects, and farm, trees nested within a farm, and sampling visit as random effects. Calculations correspond to marginal means back-transformed from the logit scale and averaged across canopy layers.

PRE-PROOF PUBLICATION

PRE-PROOF PUBLICATION JOURNAL OF PLANT PROTECTION RESEARCH

Table 2. Predicted incidence (%) of black pod and frosty pod rot according to canopy stratum.

Disease	Canopy stratum	Incidence (%) 95% CI (lower – upper)
Black pod	Lower	1.53 (0.77 - 2.99)
	Middle	3.26 (1.94 - 5.42)
	Upper	3.92 (2.34 - 6.48)
Frosty pod	Lower	13.28 (8.99 - 19.18)
	Medium	12.62 (8.57 - 18.21)
	Upper	25.08 (18.00 - 33.79)

Mean predicted incidence by canopy stratum and disease, calculated from a binomial generalized linear mixed model (GLMM) including the disease × canopy stratum interaction. Values correspond to determined marginal means (EMMeans) with 95% confidence intervals and were averaged across pod age classes.

PRE-PROOF PUBLICATION

PRE-PROOF PUBLICATION JOURNAL OF PLANT PROTECTION RESEARCH

Table 3. Mean severity (%) and 95% confidence intervals of black pod and frosty pod rot according to cacao pod developmental stage.

Disease	Pod age class	Severity (%) 95% CI
Black pod	A	0.37 (0.00–0.83)
	B	1.68 (0.93–2.44)
	C	1.20 (0.30–2.11)
	D	0.95 (0.21–1.69)
	E	5.30 (3.36–7.25)
Frosty pod rot	A	8.23 (6.10–10.40)
	B	13.20 (10.80–15.50)
	C	9.27 (6.77–11.80)
	D	6.66 (4.52–8.79)
	E	17.90 (14.30–21.50)

Severity values represent model-adjusted means determined from the cumulative link model (CLM). Pod age classes (A–E) correspond to increasing stages of pod development. Confidence intervals were calculated at the 95% confidence level.

PRE-PROOF PUBLICATION

PRE-PROOF PUBLICATION JOURNAL OF PLANT PROTECTION RESEARCH

Table 4. Mean severity (%) and 95% confidence intervals of black pod and frosty pod rot according to canopy layer.

Disease	Canopy layer	Severity (%) 95% CI
Black pod	Lower	0.75 (0.29–1.20)
	Middle	1.86 (1.13–2.58)
	Upper	2.57 (1.60–3.53)
Frosty pod rot	Lower	8.49 (6.70–10.30)
	Middle	8.91 (7.19–10.60)
	Upper	15.80 (13.50–18.20)

Severity values represent model-adjusted means determined from the cumulative link model (CLM). Lower, middle, and upper canopy layers represent the vertical strata used to evaluate disease severity within the cacao canopy. Confidence intervals were calculated at the 95% confidence level.

PRE-PROOF PUBLICATION

PRE-PROOF PUBLICATION JOURNAL OF PLANT PROTECTION RESEARCH

Table 5. Mean, standard deviation (SD), and standard error (SE) of AUDPC values for black pod disease and frosty pod rot in cacao.

Disease	AUDPC mean	SD	SE
Black pod	7.0	12.4	2.92
Frosty pod rot	14.0	13.4	3.16

AUDPC = area under the disease progress curve. Values shown correspond to descriptive statistics calculated from the observed AUDPC values before model fitting. SD = standard deviation; SE = standard error of the mean.

Table 6. Variance components of the linear mixed-effects model fitted to square-root-transformed AUDPC values.

Hierarchical level	Variance	Standard deviation	Proportion of variance (%)
Farm	1.102	1.050	19.0
Tree (nested within farm)	1.178	1.085	20.3
Residual	3.524	1.877	60.7
Total	5.804	—	100

AUDPC = area under the disease progress curve. Variance components were determined from the linear mixed-effects model fitted to square-root-transformed AUDPC values. Percentages represent the relative contribution of each variance component to the total variance.

PRE-PROOF PUBLICATION

PRE-PROOF PUBLICATION JOURNAL OF PLANT PROTECTION RESEARCH

Table 7. Global spatial autocorrelation of disease incidence deteremined using Moran's I I.

Disease	Moran's I	p-value
Black pod	≈ 0.000	0.468
Frosty pod	0.011	0.243

Moran's I was calculated using spatial weights based on k-nearest neighbors (k = 3). Spatial analyses were based on farm centroid coordinates.

Table 8. Variance components of the binomial generalized linear mixed model.

Hierarchical component	Sampling level	Variance	% of total
Tree (within farm)	Tree level	0.271	62.42
Farm	Farm level	0.019	4.37

Variance components were determined using a binomial generalized linear mixed model (GLMM). Percentages represent the relative contribution of each hierarchical sampling level to the total variance.

PRE-PROOF PUBLICATION

PRE-PROOF PUBLICATION JOURNAL OF PLANT PROTECTION RESEARCH

Table 9. Effects of climatic variables on black pod incidence determined from the binomial GLMM

Effect	Estimate (β)	Standard Error	z value	p-value
Intercept	−3.742	0.290	−12.92	<0.001
Temperature (T_c)	0.197	0.197	1.00	0.316
Relative humidity (RH_c)	0.001	0.224	0.01	0.995
Random-effect variance (tree within farm)	0.831	—	—	—
Random-effect variance (farm)	0.034	—	—	—

Fixed effects were determined using a generalized linear mixed model (GLMM) with a binomial error distribution and logit link function. Disease incidence was calculated as the proportion of diseased pods per tree and sampling visit. Temperature (T_c) and relative humidity (RH_c) were centered and scaled (mean = 0, SD = 1). Random intercepts were included for trees nested within farms to account for repeated measurements and the hierarchical structure of the sampling design. Variance components are presented on the logit scale.

PRE-PROOF PUBLICATION

PRE-PROOF PUBLICATION JOURNAL OF PLANT PROTECTION RESEARCH

Table 10. Effects of climatic variables on frosty pod rot incidence determined from the binomial GLMM.

Effect	Estimate (β)	Standard Error	z value	p-value
Intercept	−1.608	0.190	−8.48	<0.001
Temperature (T_c)	−0.208	0.086	−2.41	0.016
Relative humidity (RH_c)	−0.429	0.088	−4.91	<0.001
Random-effect variance (tree within farm)	0.158	—	—	—
Random-effect variance (farm)	0.071	—	—	—

Fixed effects were determined using generalized linear mixed model (GLMM) with a binomial error distribution and logit link function. Disease incidence was calculated as the proportion of diseased pods per tree and sampling visit. Temperature (T_c) and relative humidity (RH_c) were centered and scaled (mean = 0, SD = 1). Random intercepts were included for trees nested within farms to account for repeated measurements and the hierarchical structure of the sampling design. Variance components are presented on the logit scale.

PRE-PROOF PUBLICATION

PRE-PROOF PUBLICATION JOURNAL OF PLANT PROTECTION RESEARCH

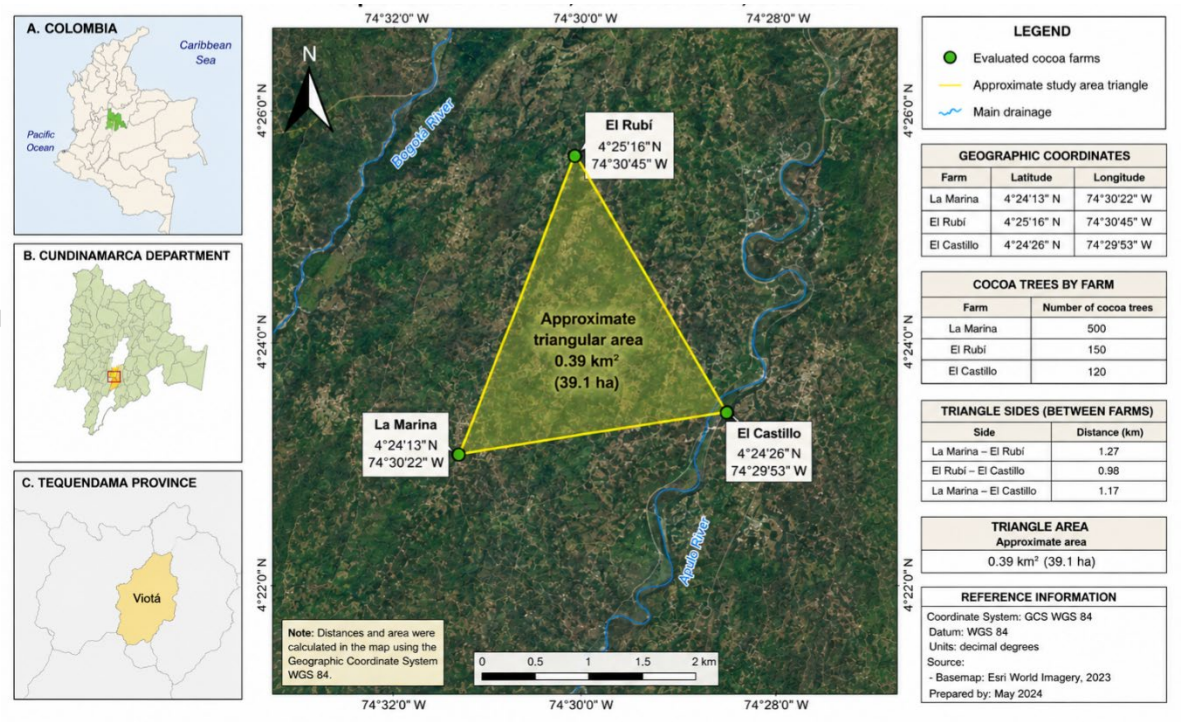


Figure 1. Geographic location of the cocoa farms included in the study in the Tequendama region, Viotá, Cundinamarca, Colombia. Figure generated with AI.



Figure 2. Pods of the developmental stages evaluated. From left to right: stage A, pods 0–10 days old; stage B, pods 10–30 days old; stage C, pods 30–60 days old; stage D, pods 60–90 days old; and stage E, pods older than 90 days.

PRE-PROOF PUBLICATION JOURNAL OF PLANT PROTECTION RESEARCH

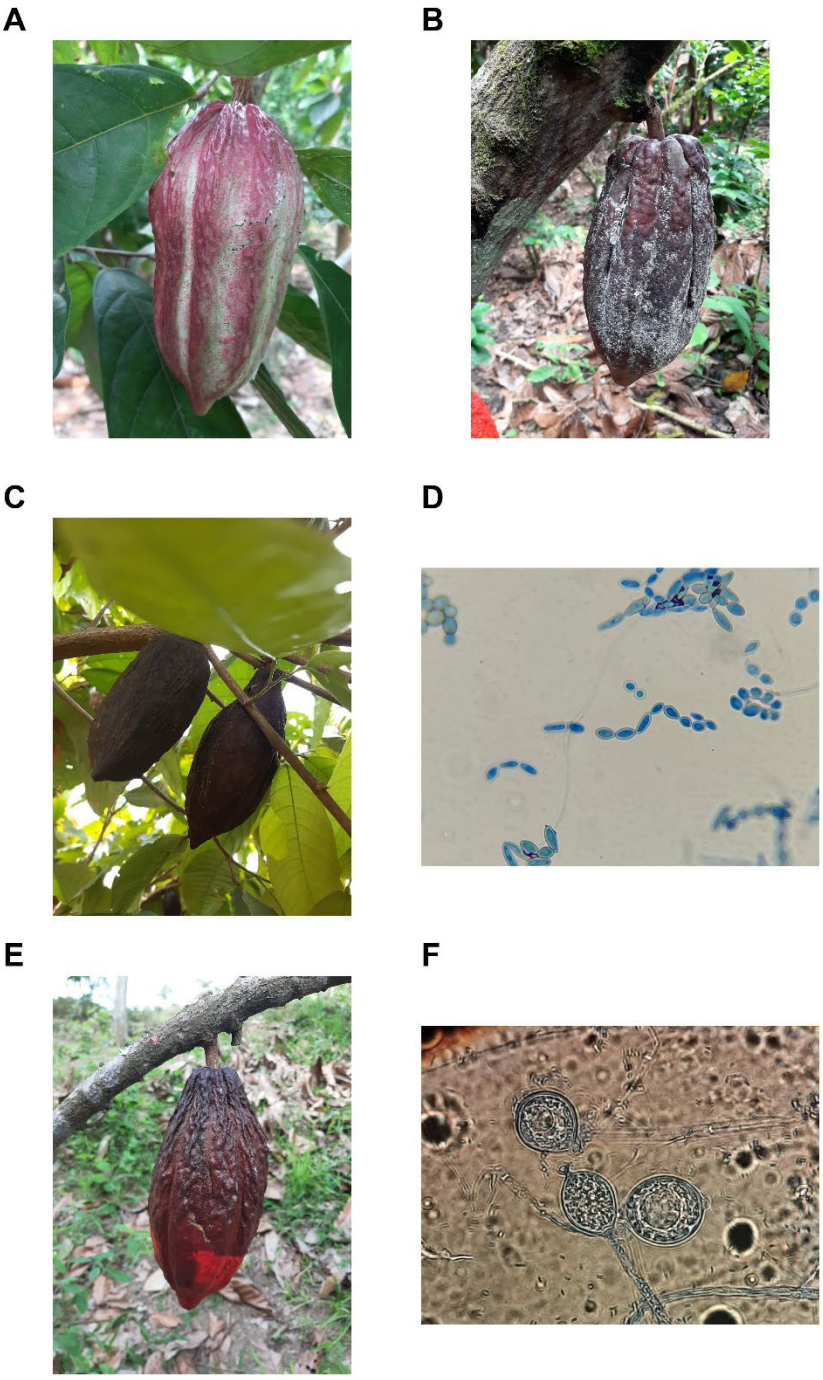


Figure 3. Pods with symptoms of frosty pod rot A) deformation of the pods (humps); B) pod with sporulation; C) Necrosis and mummification of cocoa pod; D) Sporophores of *Moniliophthora* sp; E) Black pod in cocoa; F) Sporangia of *Phytophthora* sp.

PRE-PROOF PUBLICATION JOURNAL OF PLANT PROTECTION RESEARCH

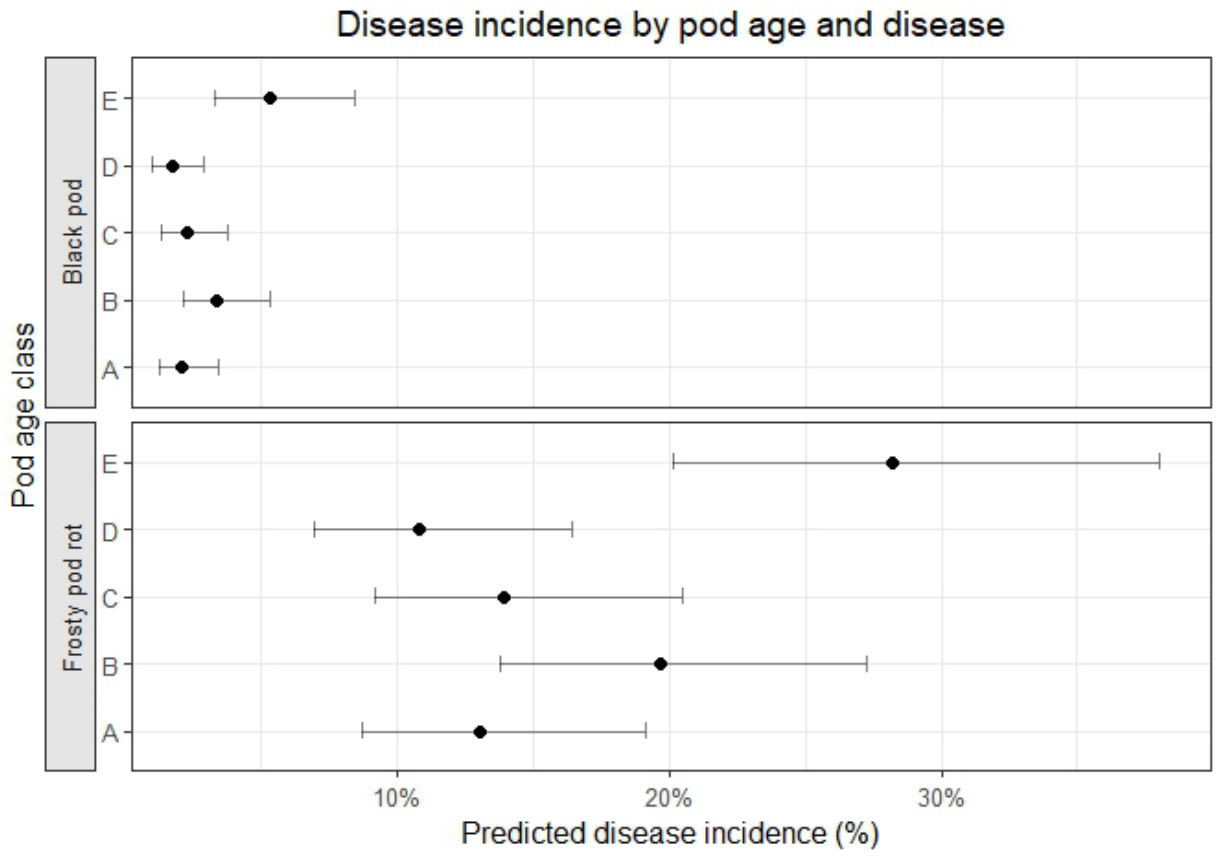


Figure 4. Calculated incidence of black pod and frosty pod rot according to pod age in cocoa. Predicted disease incidence (estimated marginal mean ± 95% confidence interval) as a function of pod age class (A–E), stratified by disease type. Values correspond to predictions on the response scale obtained from a generalized linear mixed model (GLMM) with a binomial distribution, which included fruit age and the disease × canopy stratum interaction as fixed effects, and sampling visit and tree nested within a farm as random effects. Horizontal bars represent the 95% confidence intervals, and black points indicate the estimated marginal means.

PRE-PROOF PUBLICATION JOURNAL OF PLANT PROTECTION RESEARCH

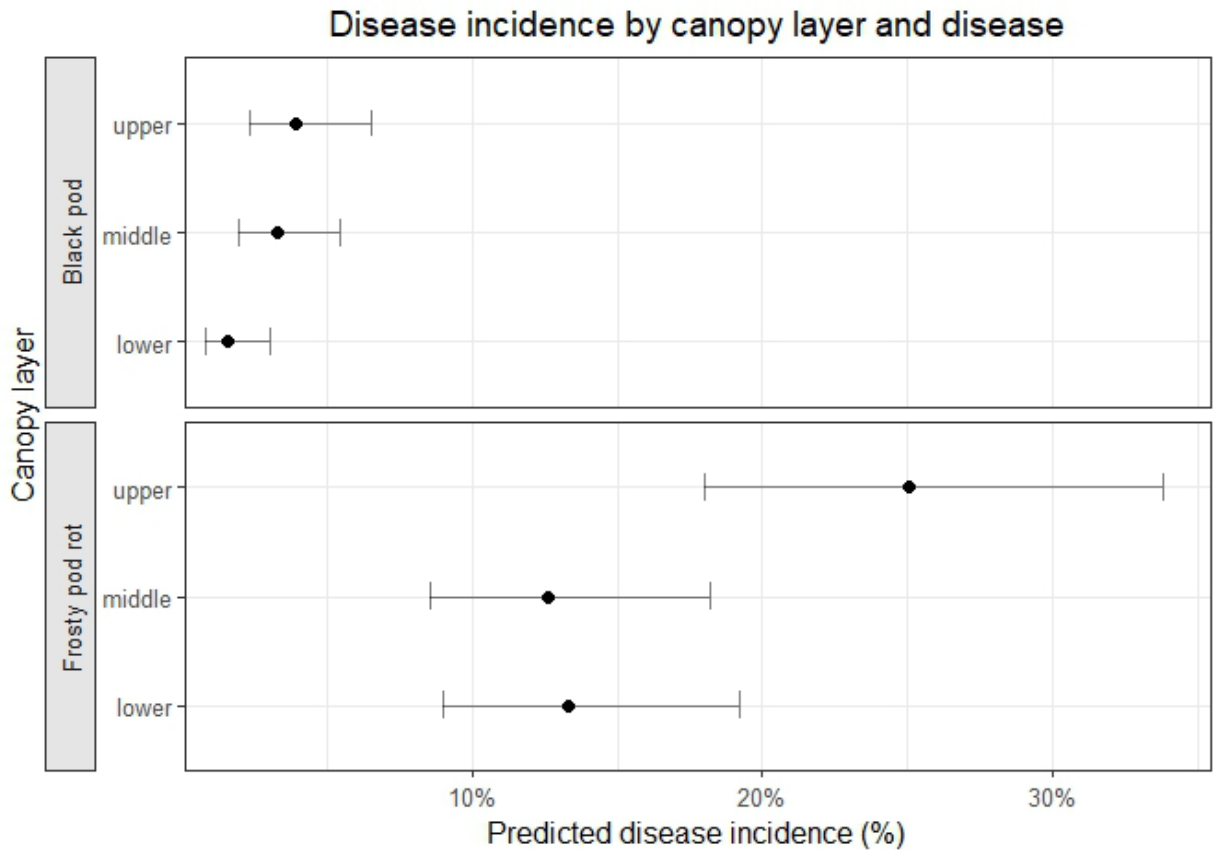


Figure 5. Predicted incidence (%) of black pod and frosty pod rot by canopy stratum

Predicted incidence of disease (estimated marginal mean ± 95% confidence interval) as a function of canopy stratum (lower, middle, and upper), stratified by disease type. The values correspond to response scale predictions obtained from a generalized linear mixed model (GLMM) with binomial distribution, which included canopy stratum and disease × canopy stratum interaction as fixed effects, and visit and tree nested within a farm as random effects. The horizontal bars represent 95% confidence intervals and the black dots indicate the calculated marginal means.

PRE-PROOF PUBLICATION JOURNAL OF PLANT PROTECTION RESEARCH

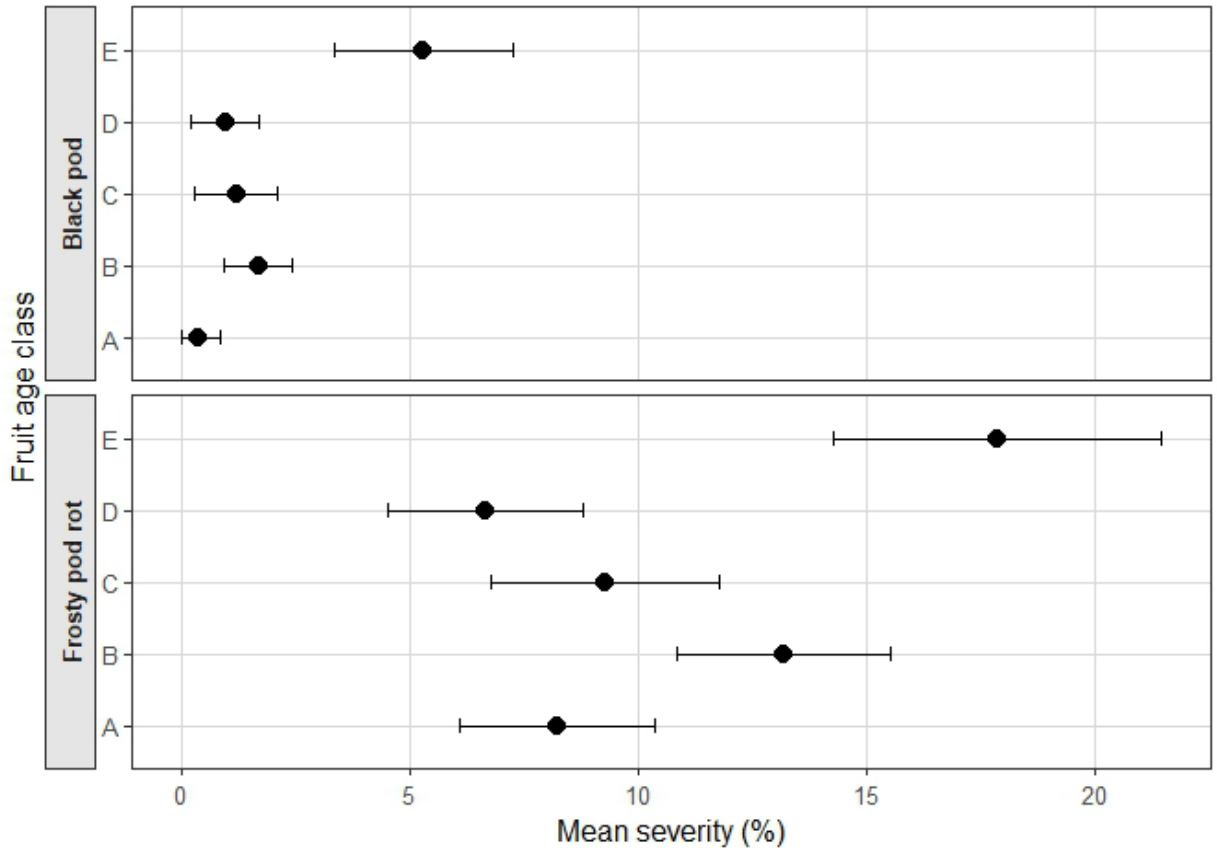


Figure 6. Mean severity (%) and 95% confidence intervals of black pod and frosty pod rot by fruit age class.

Mean disease severity (%) and 95% confidence intervals according to pod developmental stage for black pod and frosty pod rot in cacao. Severity was determined as the proportion of pod surface affected and expressed as percentage values. Points represent observed mean severity and horizontal bars indicate 95% confidence intervals. Panels correspond to evaluated disease.

PRE-PROOF PUBLICATION JOURNAL OF PLANT PROTECTION RESEARCH

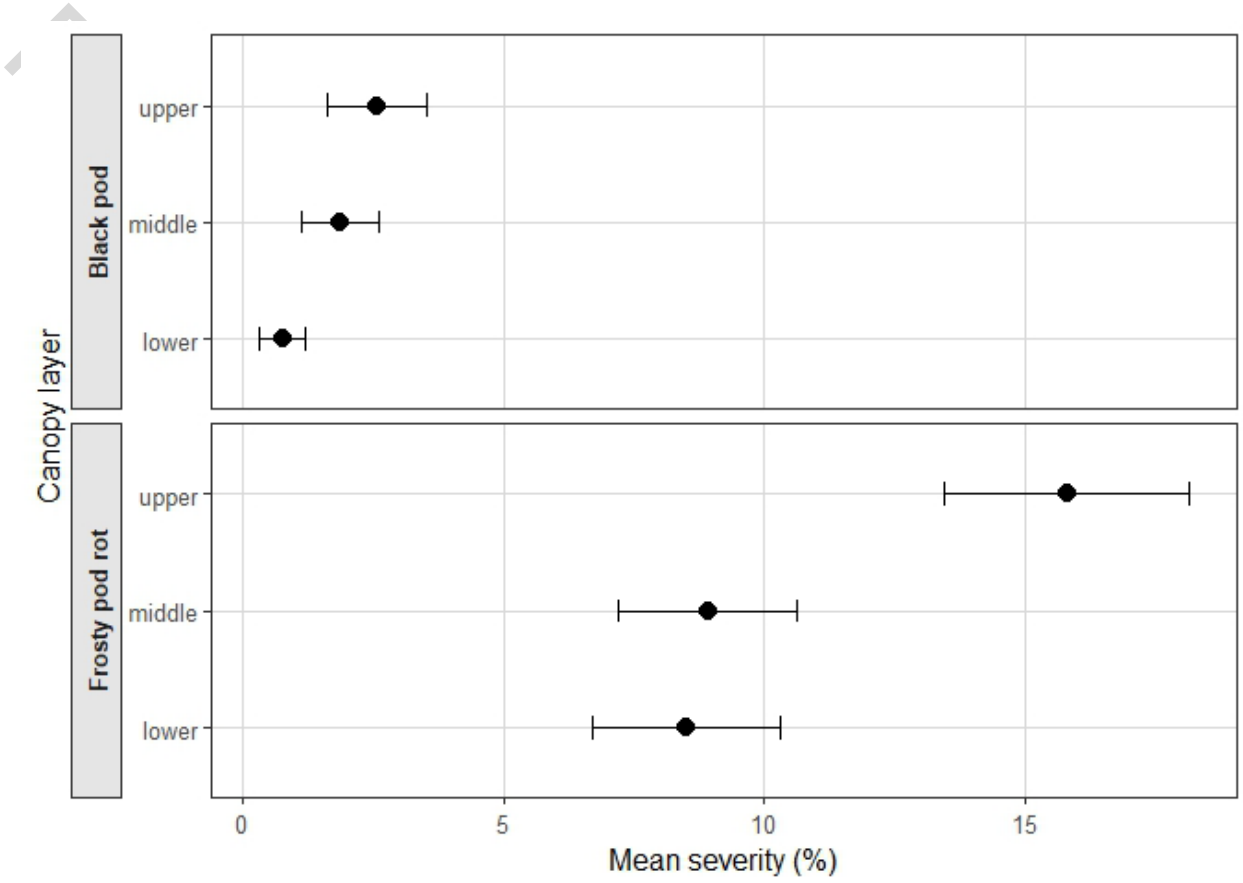


Figure 7. Mean severity (%) and 95% confidence intervals of black pod and frosty pod rot by canopy

Mean disease severity (%) and 95% confidence intervals according to canopy layer for black pod and frosty pod rot. Severity increased toward the upper canopy, particularly for frosty pod rot. Points represent observed mean severity and horizontal bars indicate 95% confidence intervals.

PRE-PROOF PUBLICATION JOURNAL OF PLANT PROTECTION RESEARCH

PRE-PROOF PUBLICATION JOURNAL OF PLANT PROTECTION RESEARCH

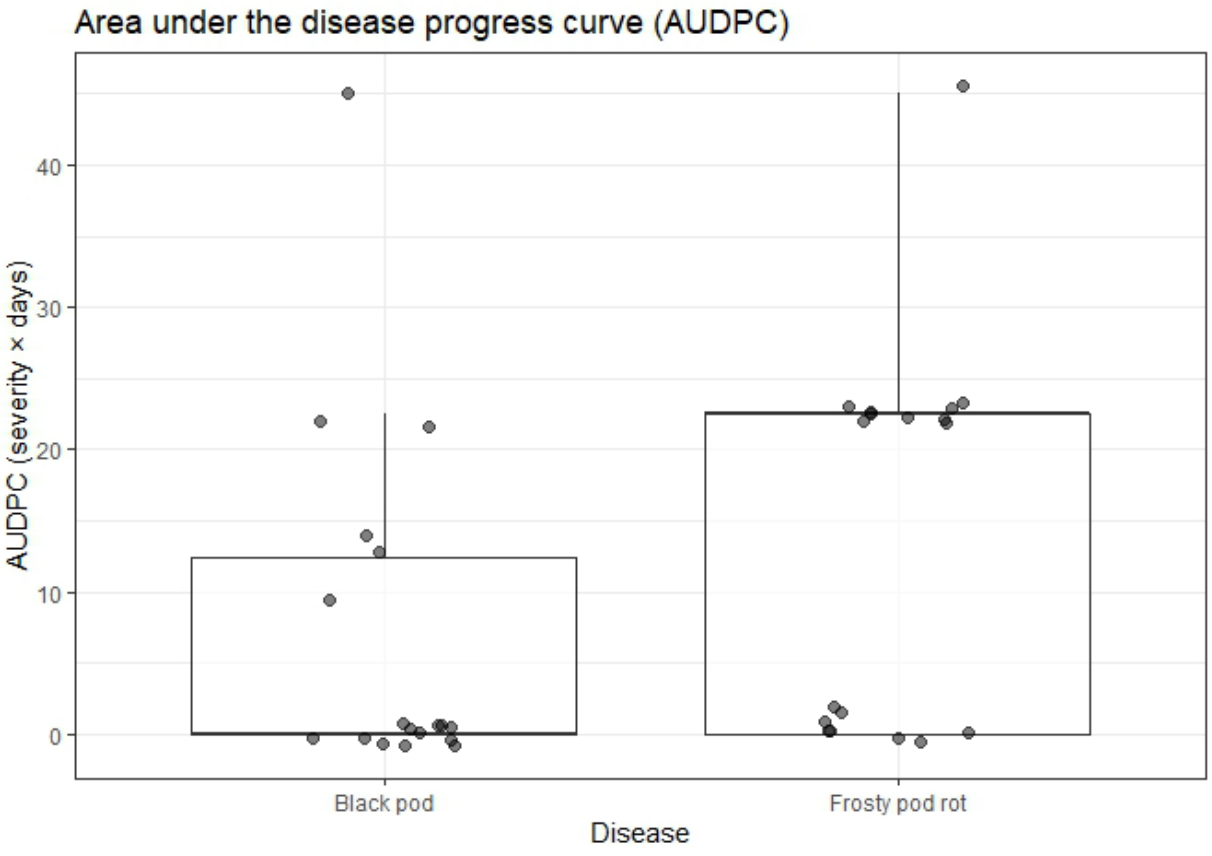


Figure 8. Area under the disease progress curve (AUDPC) for black pod and frosty pod rot in cocoa.

AUDPC was calculated from repeated severity assessments conducted at regular 45-day intervals using the trapezoidal method. Boxes represent the interquartile range (Q1–Q3), the

central line indicates the median, and whiskers correspond to 1.5 times the interquartile range. Points represent individual AUDPC values per tree. The high dispersion of values reflects heterogeneity in disease progression between trees and farms.

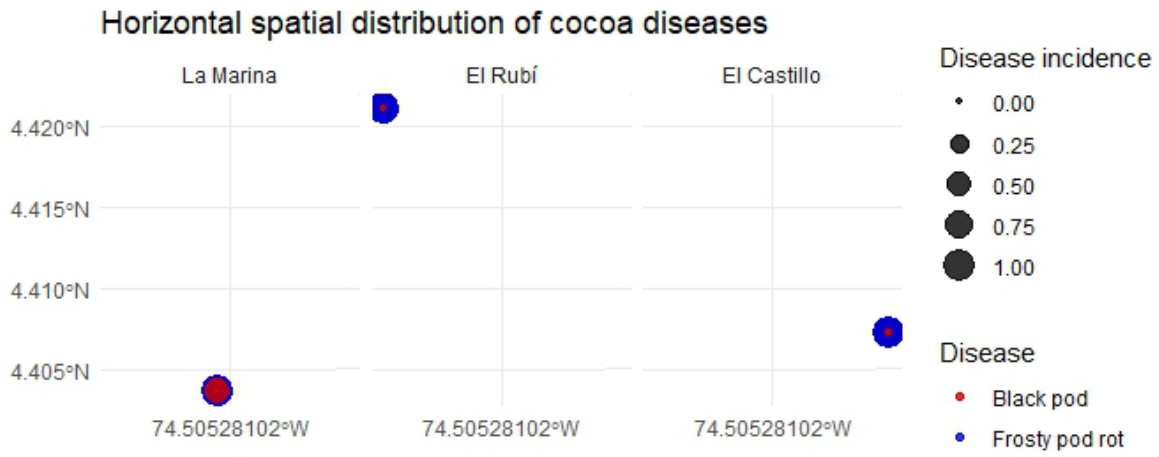


Figure 9. Horizontal distribution of black pod and frosty pod rot incidence across the cocoa farms evaluated in this study

Horizontal distribution of black pod and frosty pod rot incidence across the three cocoa farms evaluated in Viotá, Colombia. Point size is proportional to disease incidence, and colors indicate disease type. Spatial locations correspond to farm centroids and provide an exploratory visualization of disease incidence among farms.

PRE-PROOF PUBLICATION JOURNAL OF PLANT PROTECTION RESEARCH

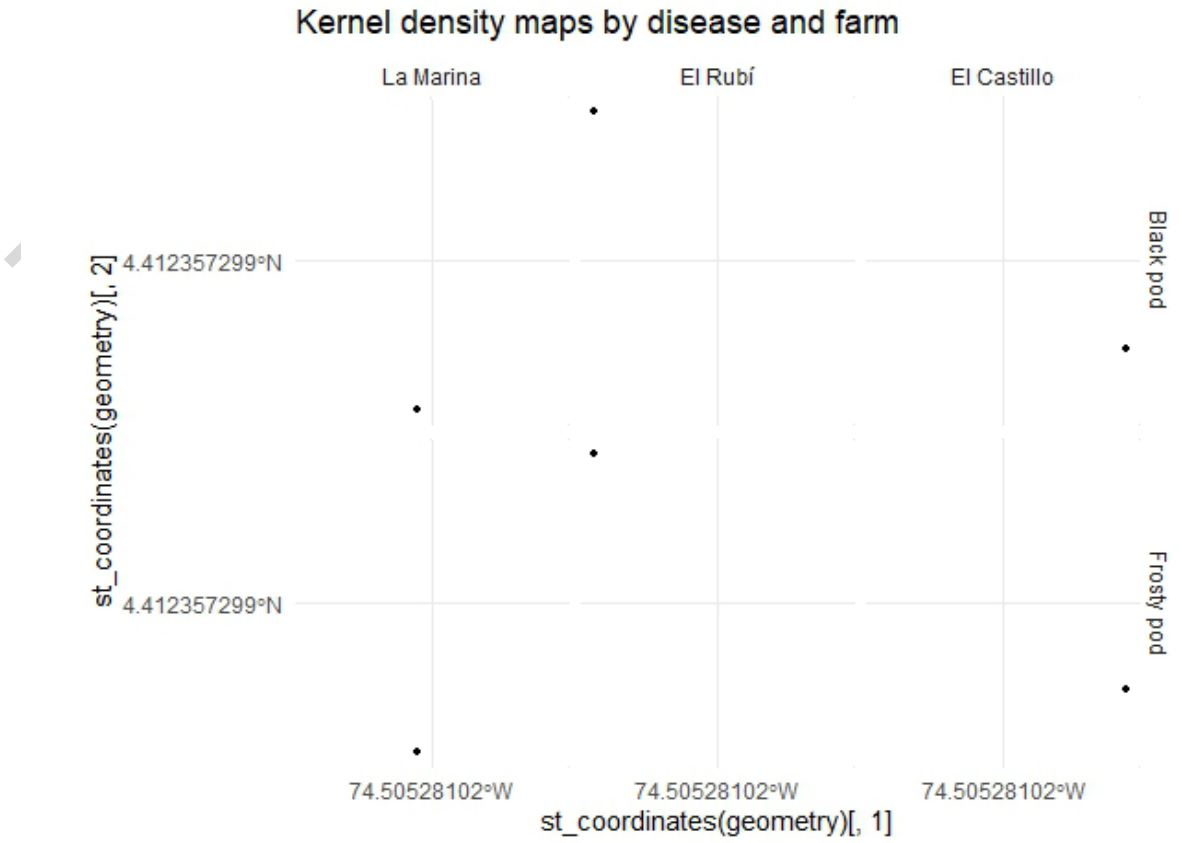


Figure 10. Spatial location of disease observations used for exploratory kernel analyses. Spatial location of black pod and frosty pod rot observations used for exploratory kernel analyses. Panels represent the three cocoa farms evaluated in the study, whereas rows correspond to disease type. Points indicate the geographic location of observations based on farm centroids.

PRE-PROOF PUBLICATION JOURNAL OF PLANT PROTECTION RESEARCH

UBLICATION